JOURNAL OF AIRCRAFT
Vol. 33, No. 3, May–June 1996

# Structural Weight Estimation for Multidisciplinary Optimization of a High-Speed Civil Transport

X. Huang,* J. Dudley,† R. T. Haftka,‡ B. Grossman,§ and W. H. Mason¶
*Virginia Polytechnic Institute and State University, Blacksburg, Virginia 24061-0203*

**A variable-complexity-modeling design strategy with combined aerodynamic and structural optimization procedures is presented for the high-speed civil transport (HSCT). A finite element model-based structural optimization procedure with flexible loads is implemented to evaluate the wing-bending material weight. Static aeroelastic effects on wing-bending material weight, evaluated through the comparison of rigid and flexible wing models, are found to be small in the HSCT design. The results of structural optimization are compared with two quasiempirical weight equations. Good correlation is obtained between the structural optimization and one of the weight equations. Based on this comparison, an interlacing procedure is developed to combine both the simple weight equations and the structural optimization in the HSCT design optimization, at modest computational cost.**

## Nomenclature

$A_e$ = derivatives of the aerodynamic loads to the elastic deformation
$A_\alpha$ = derivatives of the aerodynamic loads to $\alpha$
$b$ = wingspan, ft
$C$ = wing bending factor
$F_a$ = aerodynamic force vector
$F_g$ = gravity force vector
$F_p$ = propulsion force vector
$f_a$ = generalized aerodynamic force vector
$f_a$ = aeroelastic tailoring factor
$f_{ai}$ = component of generalized gravity force vector
$f_{a0}$ = initial generalized aerodynamic load vector
$f_c$ = composite material factor
$f_g$ = generalized gravity force vector
$f_{gf}$ = change in $f_g$ because of unit $\Delta W_f$
$f_{gi}$ = generalized gravity load caused by a unit weight in the $i$th fuel tank
$f_{gi}$ = component of generalized gravity force vector
$f_{g0}$ = generalized gravity load corresponding to a nominal set of fuel weights
$f_p$ = generalized propulsion force vector
$f_{pi}$ = component of generalized propulsion force vector
$f_{ul}$ = ultimate load factor
$K$ = stiffness matrix
$k$ = generalized stiffness matrix
$k_{ij}$ = component of generalized stiffness matrix
$M$ = mass matrix
$m$ = generalized mass matrix
$m_{ij}$ = component of generalized mass matrix
$n$ = load factor
$n_t$ = number of fuel tanks
$R_{ij}$ = correlation coefficient between data set $i$ and $j$
$s$ = interlacing factor
$u$ = displacement vector
$V$ = forward aircraft velocity
$W_b$ = wing-bending material weight, lb
$W_{fb}$ = estimated wing bending material weight from FLOPS weight equation
$W_i$ = optimum distributed weight of fuel in $i$th tank
$W_{i0}$ = nominal fuel weight in $i$th tank
$W_{ob}$ = estimated wing bending material weight from structural optimization
$\alpha$ = angle of attack
$\Delta W_f$ = amount of fuel moving aft
$\theta$ = pitch angle
$\Theta_{ec}$ = elastic shape deformation at cruise
$\Theta_j$ = jig shape of the wing
$\Theta_s$ = elastic shape deformation
$\Phi_e$ = elastic modes
$\Phi_x$ = fore/aft rigid body mode
$\Phi_z$ = plunge rigid body mode
$\Phi_\theta$ = pitch rigid body mode
$'$ = first derivatives with respect to structural design variable
$\cdot$ = first derivative with respect to time $t$ or velocity
$\cdot\cdot$ = second derivative with respect to time $t$ or acceleration

Presented as Paper 94-4379 at the AIAA/NASA/USAF/ISSMO 5th Symposium on Multidisciplinary Analysis and Optimization, Panama City Beach, FL, Sept 7–9, 1994; received Jan. 21, 1995; revision received Jan. 11, 1996; accepted for publication Jan. 16, 1996. 

*Research Engineer, Department of Aerospace and Ocean Engineering; currently at Computer Aided Technology, Inc., Livonia, MI 48152.
†Research Assistant, Department of Aerospace and Ocean Engineering. Student Member AIAA.
‡Professor, Department of Aerospace and Ocean Engineering; currently at the Department of Aerospace Engineering, Mechanics and Engineering Science, University of Florida, Gainesville, FL 32611-6250. Associate Fellow AIAA.
§Professor and Department Head, Department of Aerospace and Ocean Engineering. Associate Fellow AIAA.
¶Professor, Department of Aerospace and Ocean Engineering. Associate Fellow AIAA.

## Introduction

MULTIDISCIPLINARY optimization preserves cross-disciplinary influences in the design of aerospace vehicles, but the computational cost is often great. Variable-complexity modeling addresses this expense by coupling approximate, conceptual-level models to more advanced, detailed-level models. This approach offers the benefit of providing greater insight into the characteristics of the design space, as well as reduced computational cost, while comparing and correcting the performance predicted by simple methods with the more sophisticated techniques.[1,2]

The current problem being considered is the design of a high-speed civil transport (HSCT). We have studied the aerodynamic design of this vehicle employing a conceptual-level weight equation to account for structural weight.[3,4] However, since the HSCT is a new aircraft, the weight equation may not

account for all features of the design. Furthermore, by its nature, a weight equation can provide only a rough estimate of structural weight.[5] As shown later in this article, we found differences of the order of a factor of 2 between two weight equations. To overcome the shortcomings of weight equations we have also developed a finite element-model-based structural optimization procedure with flexible loads for estimating wing structural weight.[6]

The objective of this article is to combine the structural optimization procedure with the aerodynamic optimization procedure by using both the structural optimization and a simple weight equation together as a compromise between computational cost and accuracy. To validate this procedure, we compared the predictions of wing-weight equations with the results of structural optimization based on rigid and flexible loads. To avoid conclusions that reflect the idiosyncrasies of one particular weight equation, two different weight equations developed for NASA[7,8] are evaluated.

## Configuration Optimization

Successful optimization requires a simple, yet meaningful, mathematical characterization of the geometry. We have developed a model that defines the geometry and the aerodynamic performance using 26 design variables.[4] The wing planform is described by eight design variables and the airfoil thickness distribution with an additional five. The nacelles move axially with the wing's trailing edge, and two design variables define their spanwise locations. The axisymmetric fuselage requires eight design variables to specify the axial location and radius of the four restraint locations selected to model the baseline configuration. While the configuration is defined using this set of design variables, the aircraft geometry is actually stored as a discrete numerical description in the Craidon format.[9] In addition to the geometric design variables, three variables define the idealized cruise mission. One variable is the mission fuel and the other two specify the initial cruise altitude and the constant climb rate used in the range calculation.

The objective function is the takeoff gross weight, which is to be minimized for the specified range of 5500 nm, at Mach 2.4, with 251 passengers. There are 53 constraints, which consist of aerodynamic/performance constraints and geometric constraints. The aerodynamic/performance constraints include limits on the range, landing angle of attack, and overall lift coefficient and section lift coefficients at landing speed. The geometric constraints include bounds on the following quantities: fuel volume, leading- and trailing-edge break locations, thicknesses at several span locations, fuselage restraint locations, and nacelle locations. These geometric constraints prevent the optimizer from creating physically impossible designs.

Because the more detailed aerodynamic calculations, e.g., the Harris program for the wave drag,[10] the supersonic Mach-box-type panel method for drag caused by lift,[11] or the vortex–lattice program for landing performance, are computationally expensive, a sequential approximate optimization technique was employed in which the overall design process is composed of a sequence of optimization cycles. At the beginning of each cycle, approximations of the wave drag and drag because of lift based on simpler models are constructed. Then, the constraints of range, landing angle of attack, and lift-coefficient are calculated based on these approximations in each cycle. Move limits are imposed on the design variables to avoid large errors. After each cycle, the detailed analysis is performed and its results are used to correct the approximate models by using different methods such as linear, scaled, and global–local approximation.[4] The optimization is performed by the NEWSUMT-A program,[12] which uses a gradient-based sequential unconstrained minimization technique and an extended interior penalty function.

As is commonly done, we neglect the effects of structural deformation on aerodynamic performance, assuming that most of these are eliminated through the jig shape. With this assumption, the only interaction between the configuration and structural design is through the structural weight, which must be minimized. Performing structural optimization for each configuration is expensive, and so it is quite common to instead use approximate weight equations.

## Structural Weight Estimation

In the configuration design optimization we used the weight equations taken from the aircraft sizing program FLOPS (Ref. 7) to determine the takeoff gross weight. In particular, we use the FLOPS wing–weight equation to estimate the effect of wing geometry change on structural weight. The equation of wing bending-material weight in FLOPS can be expressed as

$$W_b = Cf_{\text{wl}}b(1 - 0.4f_c)(1 - 0.1f_a)$$

where $C$ is a factor that accounts for the effect of wing area, aspect ratio, load sweep angle, thickness-to-chord, and load distribution on the wing structural weight. The factor $C$ is calculated by approximately determining the required material volume of the upper and lower skins in a simple wing–box description of the wing for an elliptic-load distribution.[6] The average values of detailed wing geometric parameters are used to represent the simple box geometry. To compare the weight equations with the structural optimization, we need to select a wide range of configuration designs. Figure 1 gives the planforms of the 10 designs that were selected. The first design is our parametrization of the Mach 2.4 HSCT baseline design (obtained from NASA). The others are intermediate designs that we obtained in the course of several configuration optimization studies. Some of these designs are unusual, but because they are encountered in the course of configuration optimization, we must have reliable weight estimates for them.

The FLOPS weight equation was developed based on a database of existing aircraft and some optimization results. However, because of the inherent limitations of simple weight equations, we compared it to another weight equation developed by York and Labell[8] of the Grumman Aerospace Corporation. The Grumman weight equation was developed only for wing weight estimation and it uses more wing geometric parameters than does FLOPS. To provide more accurate structural weight estimates, we also implemented a finite element model-based structural optimization procedure to estimate the wing bending-material weight.

### Structural Optimization Problem

The structural optimization was performed for a fixed wing, fuselage, and nacelle configuration with titanium wing skin using a finite element model with the EAL program.[13]

The objective is to minimize the wing-skin-material weight, and the design variables define wing panel thicknesses and spar and rib cap areas. Figure 2 shows a typical distribution of the design variables for the skin panel thicknesses and the spar cap areas of one surface. For each surface 13 variables were used to define the skin panel thicknesses, and six for the

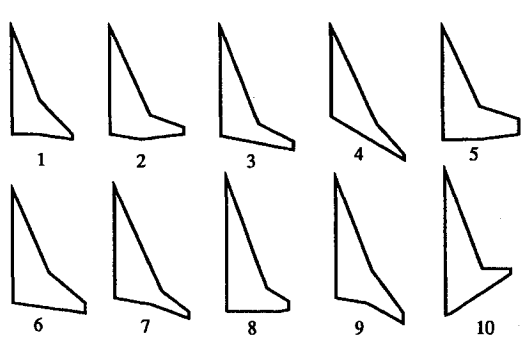


**Fig. 1 Planforms for comparison study.**

spar cap areas; only one design variable was used for the rib cap areas because they always tended to the minimum gauge. This leads to 20 design variables for each wing surface or 40 for the entire wing. We assumed a uniform thickness or area distribution within each group.

We applied von Mises stress constraints to all of the panel, spar, and rib-cap elements. Local buckling constraints were applied, assuming skin panels on the actual wing were 2.5 × 2.5 ft$^2$ and were made of sandwich construction with a 0.75-in. honeycomb core. The minimum gauge of the wing skin thickness was 0.004 ft, and the minimum spar and rib cap area was 0.005 ft$^2$.

### Modeling

Rather than manually constructing a finite element model for a given aerodynamic design, we developed a mesh generator to automate the procedure. The aerodynamic configuration is specified by the Craidon geometry description used in the configuration optimization. Besides the Craidon geometry, we need to specify the number of frames in the fuselage, the number of spars and ribs in the wing, and the chord fractions taken by the leading- and trailing-edge control surfaces. Figure 3 shows two typical finite element meshes automatically generated by this program. The left half of the figure shows the mesh for an initial design, and the right side for a final design. Besides the finite element node coordinates and element topology data, the program also estimates the locations of all nonstructural weights and the volumes and locations of the wing fuel tanks. The spar configuration generated by the program may be swept or cranked. The boundary conditions specify symmetry of the displacements about the centerline.

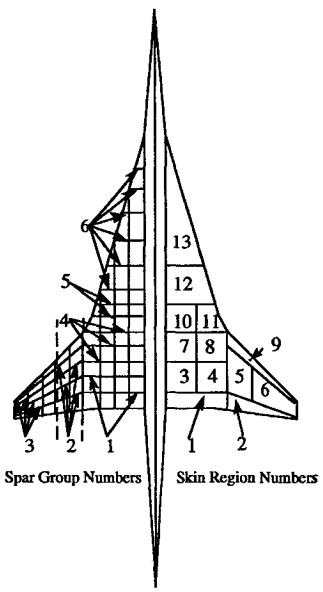


**Fig. 2 Design variables.**

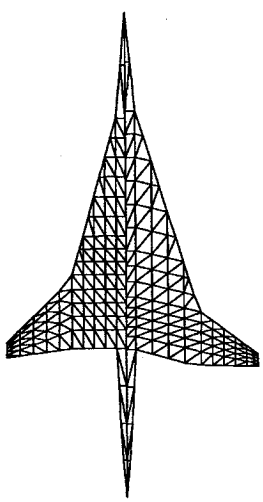

**Fig. 3 Finite element mesh from automatic model-generation program for two different planforms.**

**Table 1 Titanium properties and allowables**

| |
|---|
| $E = 16.0 \times 10^6$ psi |
| $G = 6.0 \times 10^6$ psi |
| $\nu = 0.332$ |
| $\rho = 0.163$ lb/in.$^3$ |
| $\sigma_{x_{yield}} = \sigma_{y_{yield}} = 91.8 \times 10^3$ psi |
| $\sigma_{xy_{yield}} = 53.0 \times 10^3$ psi |
| $\sigma_{x_{fatigue}} = \sigma_{y_{fatigue}} = 25.0 \times 10^3$ psi |
| $\sigma_{xy_{fatigue}} = 14.4 \times 10^3$ psi |

**Table 2 Structural load cases**

| Load case | Load factor | Mach number | Dynamic pressure, lb/ft$^2$ | Fuel weight, % |
|---|---|---|---|---|
| 1. Middle cruise | 1.0 | 2.4 | 535 | 50 |
| 2. Transonic climb | 1.0 | 1.2 | 644 | 90 |
| 3. Low-speed pull-up | 2.5 | 0.6 | 367 | 95 |
| 4. High-speed pull-up | 2.5 | 2.4 | 723 | 80 |
| 5. Taxiing | 1.5 | 0.0 | 0 | 100 |

### Material and Loads

Titanium was used for all structural components. Its properties and allowables are given in Table 1.

Following Ref. 14, we considered five different load cases in the optimization, as shown in Table 2. Load cases 1 and 2 have a 1.5 safety factor for stress and strain and a 1.5 safety factor for buckling. Load cases 3, 4, and 5 have a 1.5 safety factor for stress and strain, and a safety factor of 2.25 for buckling.

## Flexible-Load Calculation

To take into account static aeroelastic effects, we implemented a flexible-load-generation program. Trimming for pitch by fuel management is also included in the program. In the formulation presented next, the elastic deformation of the structure is treated in a quasistatic method. We assume that the angle of pitch is small and the forces related to the velocity of $\dot{\theta}$ are negligible. We only consider symmetric cruise and maneuver conditions.

### Aeroelastic Formulation

The equation of motion of an aircraft discretized by a finite element model is

$$M\ddot{u} + Ku = F_a + F_g + F_p \tag{1}$$

The vector $u$ combines both rigid body motion and elastic deformations. To reduce the cost of analysis we use the vibration modes $\Phi_e$ to approximate the elastic component of the displacement vector, and $u$ can be expressed as

$$u \cong \Phi_z u_z + \Phi_\theta \theta + \Phi_x u_x + \Phi_e \Theta_e \tag{2}$$

where $\Phi_z$, $\Phi_\theta$, $\Phi_x$, and $\Phi_e$ are the plunge, pitch, fore/aft rigid body modes, and elastic modes, respectively. By using this modal approximation, a system with thousands of degrees of freedom is typically reduced to about 20 or 30 modal coordinates. Here, $\Phi_e$ may represent mode shapes of some nominal structure rather than of the structure of the current design cycle. So $\Phi_e$ is not necessarily orthonormal with respect to the mass and stiffness matrices. The option of keeping $\Phi_e$ constant

when we modify the structure can substantially improve computational efficiency.

For the inertia forces we neglect the acceleration associated with the elastic deformations, that is, treat these in a quasistatic manner, so that

$$\ddot{\boldsymbol{u}} \cong \Phi_z \ddot{u}_z + \Phi_\theta \ddot{\theta} + \Phi_x \ddot{u}_x \tag{3}$$

Substituting back into Eq. (1), we get

$$M\Phi_z \ddot{u}_z + M\Phi_\theta \ddot{\theta} + M\Phi_x \ddot{u}_x + K\Phi_e \Theta_e = \boldsymbol{F}_a + \boldsymbol{F}_g + \boldsymbol{F}_p \tag{4}$$

We premultiply Eq. (4) by $\Phi_z$, $\Phi_\theta$, $\Phi_x$, and $\Phi_e$, respectively, and define $m_{ij} = \Phi_i^T M \Phi_j$, to obtain

$$m_{zz}\ddot{u}_z + m_{z\theta}\ddot{\theta} = f_{az} + f_{gz} + f_{pz} \tag{5}$$

$$m_{z\theta}\ddot{u}_z + m_{\theta\theta}\ddot{\theta} + m_{\theta x}\ddot{u}_x = f_{a\theta} + f_{g\theta} + f_{p\theta} \tag{6}$$

$$m_{\theta x}\ddot{\theta} + m_{xx}\ddot{u}_x = f_{ax} + f_{px} \tag{7}$$

$$m_{ze}^T \ddot{u}_z + m_{\theta e}^T \ddot{\theta} + m_{xe}^T \ddot{u}_x + k_{ee}\Theta_e = f_{ae} + f_{ge} + f_{pe} \tag{8}$$

The propulsion force $f_p$ is assumed to be constant and given, and $f_a$ is assumed to depend linearly on the wing deformations and $\alpha$ as

$$f_a \cong f_{a0} + q[A_\alpha \theta + A_e(\Theta_e - \Theta_{ec})] \tag{9}$$

where $A_\alpha$ and $A_e$ are matrices of derivatives of the aerodynamic loads with respect to $\alpha$ and the elastic deformations, respectively, and $f_{a0}$ is the aerodynamic load vector at an angle of attack of $-\dot{u}_z/V$. The angle of attack is related to $\theta$ and $V$ as

$$\alpha = \theta - (\dot{u}_z/V) \tag{10}$$

The $\Theta_s$ is given as

$$\Theta_s = \Theta_e + \Theta_j \tag{11}$$

where $\Theta_j$ is built to correct for elastic deformations in some other flight condition. In this work $\Theta_j$ is assumed to correct for displacements at middle cruise (load case 1), so that $\Theta_j = -\Theta_{ec}$.

The vertical acceleration is given as $\ddot{u}_z = (n-1)g$, and we have

$$m_{zz}\ddot{u}_z = -(n-1)f_{gz} \tag{12}$$

$$m_{z\theta}\ddot{u}_z = -(n-1)f_{g\theta} \tag{13}$$

$$m_{ze}^T \ddot{u}_z = -(n-1)f_{ge} \tag{14}$$

Using Eqs. (9) and (12–14), Eqs. (5–8) may be rewritten as a set of linear equations

$$m_{z\theta}\ddot{\theta} = f_{az0} + q[A_{z\alpha}\theta + A_{ze}(\Theta_e - \Theta_{ec})] + nf_{gz} + f_{pz} \tag{15}$$

$$m_{\theta\theta}\ddot{\theta} + m_{\theta x}\ddot{u}_x = f_{a\theta 0} + q[A_{\theta\alpha}\theta + A_{\theta e}(\Theta_e - \Theta_{ec})] + nf_{g\theta} + f_{p\theta} \tag{16}$$

$$m_{\theta x}\ddot{\theta} + m_{xx}\ddot{u}_x = f_{ax0} + q[A_{x\alpha}\theta + A_{xe}(\Theta_e - \Theta_{ec})] + f_{px} \tag{17}$$

$$m_{\theta e}^T \ddot{\theta} + m_{xe}^T \ddot{u}_x + k_{ee}\Theta_e = f_{ae0} + q[A_{e\alpha}\theta + A_{ee}(\Theta_e - \Theta_{ec})] + nf_{ge} + f_{pe} \tag{18}$$

**Fuel Management**

The high-speed civil transport configurations we are considering at this stage have no horizontal tail, and we assume that the longitudinal trim of the aircraft is accomplished by moving fuel among the various fuel tanks. For the cruise conditions this requires a fuel management procedure to balance the aircraft in straight and level, steady flight at a given Mach number and dynamic pressure.

We assume that cruise elastic deformations are corrected through the jig shape for an average cruise condition. Neglecting variations in structural deformations during cruise, $f_a$ is a linear function of $\theta$, and does not depend on the wing deformations. The gravity load $f_g$ may be written as

$$f_g = f_{g0} + \sum_{i=1}^{n_t} (W_i - W_{i0}) f_{gi} \tag{19}$$

where $f_{g0}$ is the load corresponding to a nominal set of fuel weights $W_{i0}$ in $n_t$ fuel tanks, $f_{gi}$ is the gravity load caused by a unit weight in the $i$th fuel tank, and $W_i$ is the actual weight of fuel in $i$th tanks. For cruise $n = 1$ and $\ddot{\theta} = \ddot{u}_x = \ddot{u}_z = 0$, and Eqs. (15–18) may be simplified as

$$f_{az0} + qA_{z\alpha}\theta + f_{gz} + f_{pz} = 0 \tag{20}$$

$$f_{a\theta 0} + qA_{\theta\alpha}\theta + f_{g\theta} + f_{p\theta} = 0 \tag{21}$$

$$f_{ax0} + qA_{x\alpha}\theta + f_{px} = 0 \tag{22}$$

$$k_{ee}\Theta_{ec} = f_{ae0} + qA_{e\alpha}\theta + f_{ge} + f_{pe} \tag{23}$$

Equation (20) defines the lift requirement and is used to calculate the required $\theta$ (hence, angle of attack). Equation (21) is the pitch equilibrium equation and constitutes a constraint on the fuel weight distribution. Equation (22) defines the thrust requirement. Since there are many ways to distribute the fuel, we define an optimization problem that seeks the fuel distribution closest to a nominal one

Minimize:

$$\sum_{i=1}^{n_t} (W_i - W_{i0})^2$$

Subject to:

$$\sum_{i=1}^{n_t} (W_i - W_{i0}) = 0$$

$$f_{a\theta 0} + qA_{\theta\alpha}\theta + f_{g\theta} + f_{p\theta} = 0$$

$$0 \le W_i \le W_i^{\max}$$

After this optimization is performed using NEWSUMT-A, Eq. (23) is used to calculate the cruise structural deformations.

**Sensitivity Calculation**

For convenience we discuss sensitivity with respect to a single structural parameter $s$. The process of derivative calculation begins with the cruise condition. To obviate the need for solving the fuel optimization problem every time we change the structure, and to simplify derivative calculation, we assume that we move fuel only between the foremost and rearmost available tanks. For this case, Eq. (19) may be written as

$$f_g = f_{g0} + \Delta W_f f_{gf} \tag{24}$$

In this case, the fuel management optimization problem re-

duces to solving the pitch equilibrium constraint equation for $\Delta W_f$:

$$f_{a\theta 0} + qA_{\theta\alpha}\theta + f_{p\theta} + f_{g\theta 0} + \Delta W_f f_{g\theta f} = 0 \quad (25)$$

To start the sensitivity calculation, we differentiate Eqs. (20) and (25) with respect to the structural design variable $s$, using a prime to denote derivatives with respect to $s$:

$$qA_{z\alpha}\theta' + f'_{gz0} + \Delta W'_f f_{gzf} = 0 \quad (26)$$

$$qA_{\theta\alpha}\theta' + f'_{g\theta 0} + \Delta W'_f f_{g\theta f} = 0 \quad (27)$$

We can solve Eqs. (26) and (27) for $\theta'$ and $\Delta W'_f$. Next, we differentiate Eq. (23) to get

$$k_{ee}\Theta'_{ec} = qA_{e\alpha}\theta' + f'_{ge0} + \Delta W'_f f_{gef} - k'_{ee}\Theta_{ec} \quad (28)$$

from which we can calculate the derivative of the cruise displacement vector $\Theta_{ec}$. Then we differentiate Eqs. (9) and (15–18) to get

$$f'_a = qA_\alpha\theta' + qA_e(\Theta'_e - \Theta'_{ec}) \quad (29)$$

$$m_{z\theta}\ddot{\theta}' - qA_{z\alpha}\theta' - qA_{ze}\Theta'_e = -m'_{z\theta}\ddot{\theta} + nf'_{gz} - qA_{ze}\Theta'_{ec} \quad (30)$$

$$m_{\theta\theta}\ddot{\theta}' + m_{\theta x}\ddot{u}'_x - qA_{\theta\alpha}\theta' - qA_{\theta e}\Theta'_e = -m'_{\theta\theta}\ddot{\theta} - m'_{\theta x}\ddot{u}_x + nf'_{g\theta} - qA_{\theta e}\Theta'_{ec} \quad (31)$$

$$m_{\theta x}\ddot{\theta}' + m_{xx}\ddot{u}'_x - qA_{x\alpha}\theta' - qA_{xe}\Theta'_e = -m'_{\theta x}\ddot{\theta} - m'_{xx}\ddot{u}_x - qA_{xe}\Theta'_{ec} \quad (32)$$

$$m^T_{\theta e}\ddot{\theta}' + m^T_{xe}\ddot{u}'_x - qA_{e\alpha}\theta' - (qA_{ee} - k_{ee})\Theta'_e = -m'^T_{\theta e}\ddot{\theta} - m'^T_{xe}\ddot{u}_x + nf'_{ge} - qA_{ee}\Theta'_{ec} - k'_{ee}(\Theta_e - \Theta_{ec}) \quad (33)$$

In Eqs. (30–33) $f'_a$ is substituted from Eq. (29), and $f'_g$ has a structural component plus a fuel component obtained by solving Eqs. (26) and (27). Equations (30–33) are very similar to Eqs. (15–18), and can be solved directly.

### Implementation

The structural and nonstructural weights, except for the weight of wing-bending material, were calculated by FLOPS weight equations and redistributed to the finite element nodes. We assume that the fuel is stored in 31 tanks: 3 in the aft section of the fuselage and 14 tanks in each wing. An initial fuel distribution is used for the calculation of the mass matrix.

Aerodynamic loads are generated on the wing using the same codes that were developed for the aerodynamic optimization. That is, the loads in supersonic flight are determined from a supersonic panel method, and loads in subsonic flight from a vortex–lattice method. The aerodynamic influence coefficients, $A_\alpha$ and $A_e$ in Eq. (9), are calculated by finite differences. In the aerodynamic design we did not specify a wing camber distribution, and assumed that camber could be used to attain the performance estimated from Carlson attainable leading-edge suction theory.[11] For structural loads, however, the wing camber and twist affects the aerodynamic load distribution directly. We use Carlson's WINGDES program (Ref. 15) to generate a wing cambered for optimum cruise and compute the loads corresponding to this camber at the various flight conditions. The aerodynamic and inertia loads of the rigid-wing model are treated as a special case when the wing deformation equals zero.

## Structural Optimization Results

The structural optimization was performed using sequential linear programming, with typical initial move limits of 20%. To ensure that the weight taken from the finite element model was only that used to support bending loads, we subtracted the weight used in the control surface regions of the wing and that of the panels at minimum gauge thickness.

### Comparison of Rigid and Flexible Wing Models

The structural optimization procedure was applied to the Mach 2.4 baseline design with both rigid and flexible loads. The convergence history of the wing bending material weight for this design is given in Fig. 4. The move limits were reduced in the course of optimization, and the optimization was stopped when the weight change from one cycle to the next was small, and no constraints were violated. As can be seen, the static aeroelastic effect on the structural weight is small. To compare the final designs, the skin thickness distributions and active load cases for both rigid and flexible model designs are given in Figs. 5 and 6. The $b$ in Fig. 6 indicates that the buckling constraint is active in the marked region. The two final thickness distributions are very similar and only load cases 2 and 3 control the design variables.

To check whether the static aeroelastic effect on design loads is small in other cases, we also optimized several other designs. The largest difference in final wing bending material weights was about 7%. According to our comparison, the structural optimization based on the rigid loads appears to be a conservative estimate of the effect of the geometric changes on the structural weight.

### Comparison of Weight Equations with Structural Optimization

We applied the structural optimization with rigid loads to all of the designs shown in Fig. 1. Figure 7 summarizes the structural optimization results and the estimates of the FLOPS and Grumman weight equations for the 10 designs. The average wing bending material weights predicted by the structural optimization, FLOPS, and Grumman weight equations are 38,017, 32,454, and 45,848 lb, respectively. However, the ratios of the weight predicted by structural optimization to the FLOPS weight equation vary between 0.93–1.50, whereas the ratios between the weight predicted by structural optimization and that of Grumman weight vary between 0.59–1.18.

Since optimization is concerned with the changes in weight because of changes in geometry, we also calculated the correlation coefficients between the two weight equations and the structural optimization procedure. These correlation coefficients between two sets of data measure the extent that they increase or decrease in synchrony. We found that the values of the three correlation coefficients were $R_{FG} = -0.05$, $R_{FS} = 0.78$, and $R_{GS} = -0.34$, where $R_{FG}$ means correlation coefficient between FLOPS and Grumman weight equations, $R_{FS}$ the correlation coefficient between FLOPS and structural optimization, and $R_{GS}$ the correlation coefficient between Grumman and structural optimization. The three factors indicate that the FLOPS weight equation agrees with the structural optimization

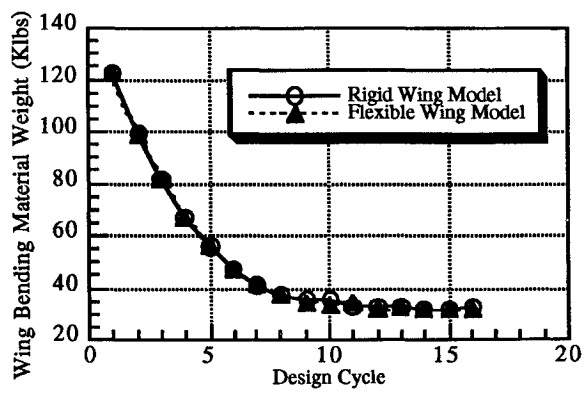


**Fig. 4 Wing-bending material weight convergence for M2.4 baseline design.**

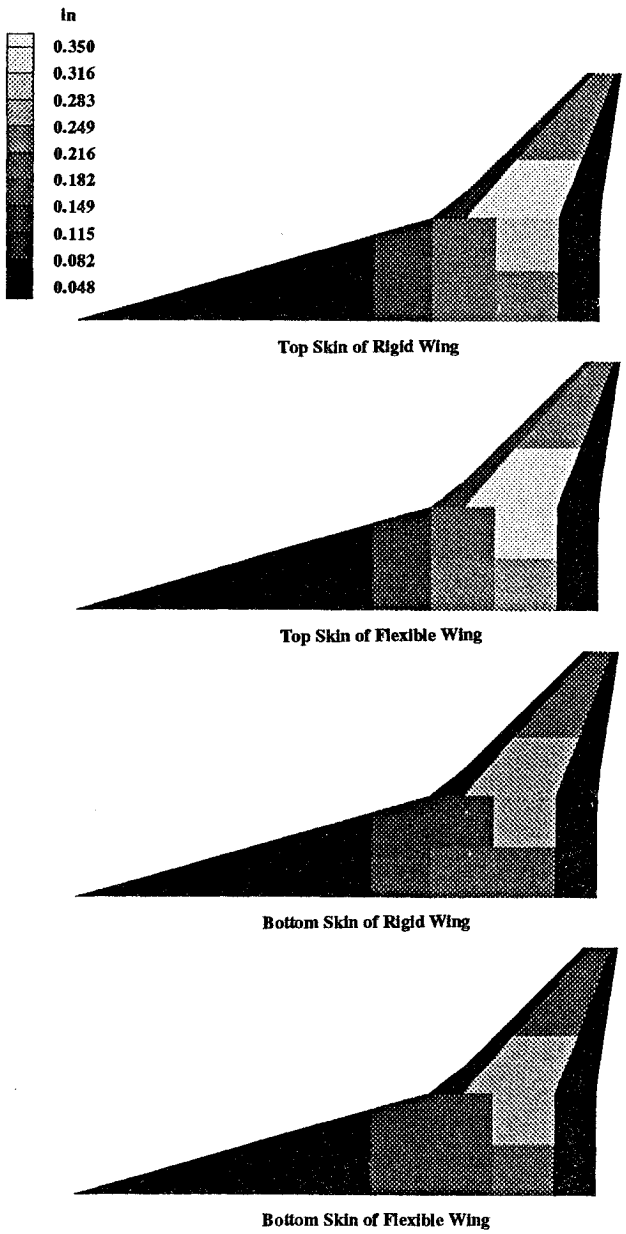


**Fig. 5 Skin thickness distribution for M2.4 baseline design.**

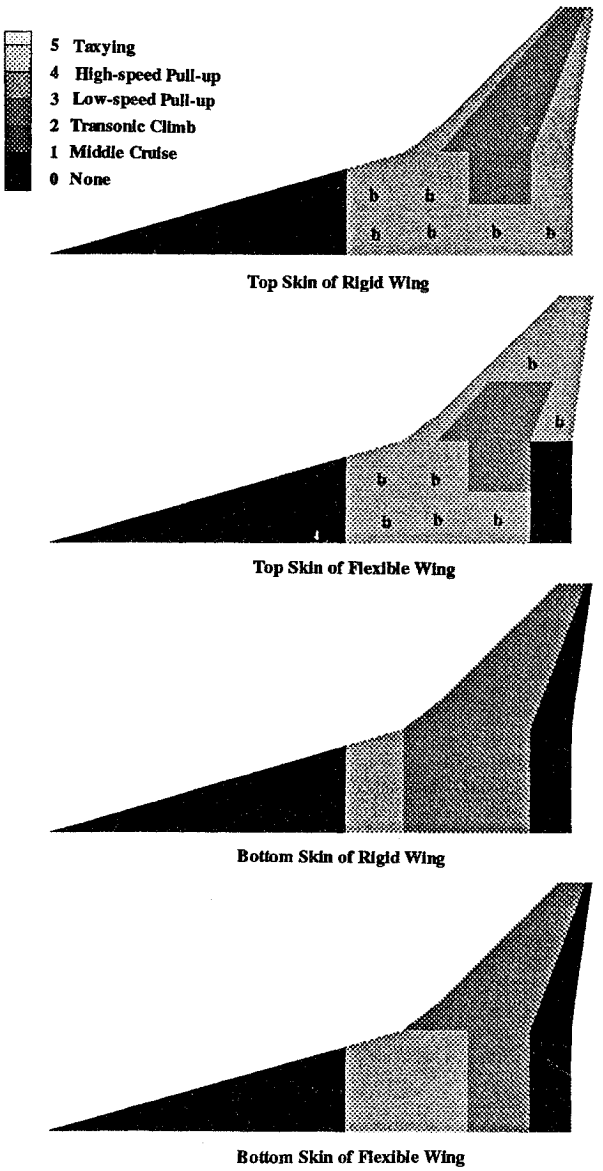


**Fig. 6 Active load cases for M2.4 baseline design.**

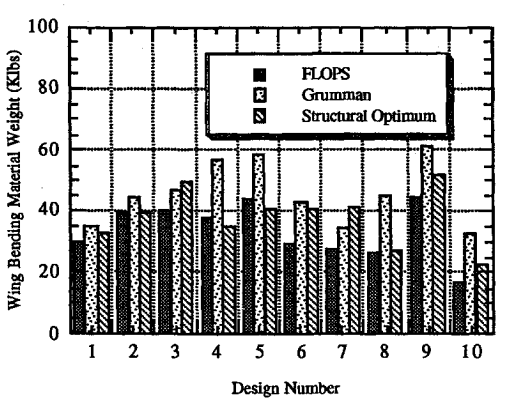


**Fig. 7 Comparison of wing-bending material weight.**

results much better than the Grumman weight equation as to the effect of geometry changes on the weight.

## Interlacing Procedure

Aerodynamic design optimization with a structural weight equation captures the major effects of aerodynamic shape on structural weight. Weight equations cannot account for all features of a new design such as the HSCT. On the other hand, finite element model-based structural optimization procedures can overcome this deficiency, but are much more expensive in comparison with the statistical-based weight equation and can only provide the structural part of the aircraft gross weight. A full integration of the structural and aerodynamic optimization is computationally expensive because of repeated calculation of aerodynamic loads and derivatives of these loads with respect to all of the aerodynamic design variables. As an intermediate step, we have implemented a variable-complexity strategy to interlace the aerodynamic and structural optimizations.

We applied the structural optimization procedure and FLOPS weight equation to the initial aerodynamic design to get $W_{fb}$, $W_{ob}$, and $s = W_{ob}/W_{fb}$. Then we started the aerodynamic design optimization by using the FLOPS weight equation with the wing bending material weight multiplied by $s$. The factor $s$ was updated periodically by repeating the structural optimization every five cycles of the aerodynamic design optimization procedure. This procedure was repeated until the design converged.

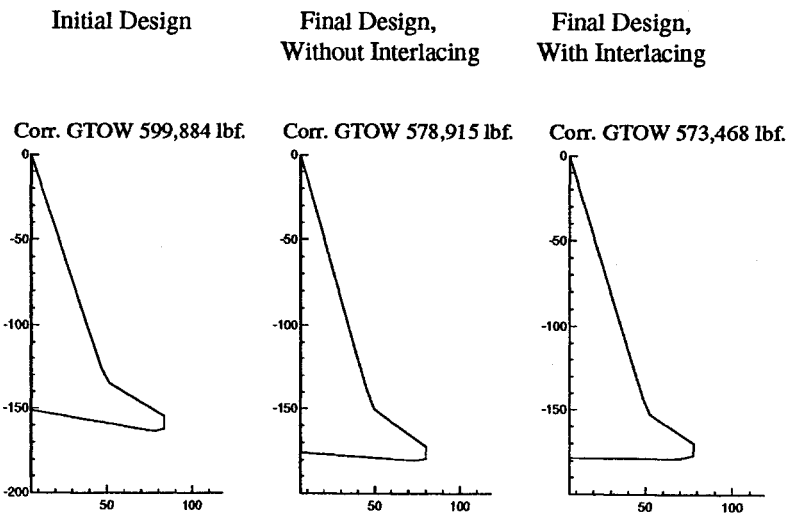


**Fig. 8 Planforms, case 1 (all dimensions in ft).**

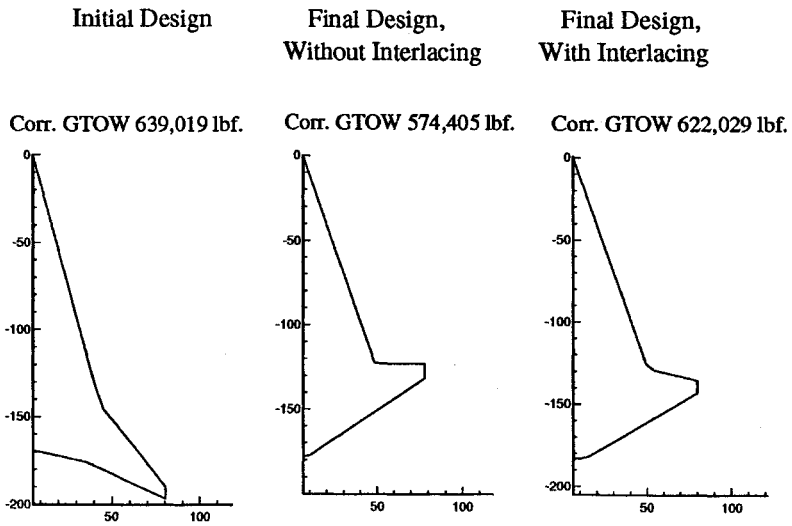


**Fig. 9 Planforms, case 2 (all dimensions in ft).**

**Table 3 Selected design parameters, case 1**

| Design parameters | Starting design | Optimization design without interlacing | Optimization design with interlacing |
|---|---|---|---|
| GTOW, lbf | 599,884 | 578,915 | 573,468 |
| Wing weight, lbf | 97,363 | 97,123 | 98,821 |
| Fuel weight, lbf | 289,990 | 280,274 | 271,980 |
| *t/c* at root, % | 2.58 | 2.56 | 2.25 |
| (*L/D*)max | 10.01 | 9.99 | 10.35 |
| Landing angle | 12.38 | 11.92 | 11.99 |
| Interlacing factor | 1.010 | 0.972 | 0.998 |

**Table 4 Selected design parameters, case 2**

| Design parameters | Starting design | Optimization design without interlacing | Optimization design with interlacing |
|---|---|---|---|
| GTOW, lbf | 639,019 | 574,405 | 622,029 |
| Wing weight, lbf | 110,881 | 89,411 | 105,959 |
| Fuel weight, lbf | 320,947 | 285,844 | 310,907 |
| *t/c* at root, % | 2.44 | 2.30 | 2.83 |
| (*L/D*)max | 11.10 | 9.74 | 9.83 |
| Landing angle | 12.58 | 11.92 | 12.00 |
| Interlacing factor | 1.169 | 1.391 | 1.501 |

## Interlacing Results

The interlacing procedure described previously was applied to two different initial designs, each of which was first optimized with FLOPS weight equation alone. Figures 8 and 9 each show the initial design, the optimum design without interlacing, and the optimum design with interlacing for cases 1 and 2, respectively. Because approximate models are used in the configuration optimization, the final design may not satisfy exactly the range constraint evaluated with the detailed models. Since the gross weight is quite sensitive to the range requirement, any range deficiency, i.e., a range of less than 5500 n mile, is corrected by the addition of an appropriate amount of fuel weight to the takeoff gross weight. This fuel weight is also used at the start of the next global iteration cycle.

Some important design characteristics are compared in Tables 3 and 4. These two cases represent a phenomenon repeatedly encountered in the configuration optimization. Noisy aerodynamic drag calculations[16] created multiple local optima in design space so that final designs were strongly dependent on initial designs. Case 1 produced an arrow–wing design and the weight equation predicted weights that were very close to those obtained by structural optimization. The interlacing procedure resulted in a slightly better design. In case 2, both with and without interlacing, the optimizer moved to an unusual planform. On the basis of the weight equation alone, the final design without interlacing appeared to be structurally superior to case 1. However, the interlacing process revealed that the optimizer took advantage of weaknesses in the FLOPS weight equations.

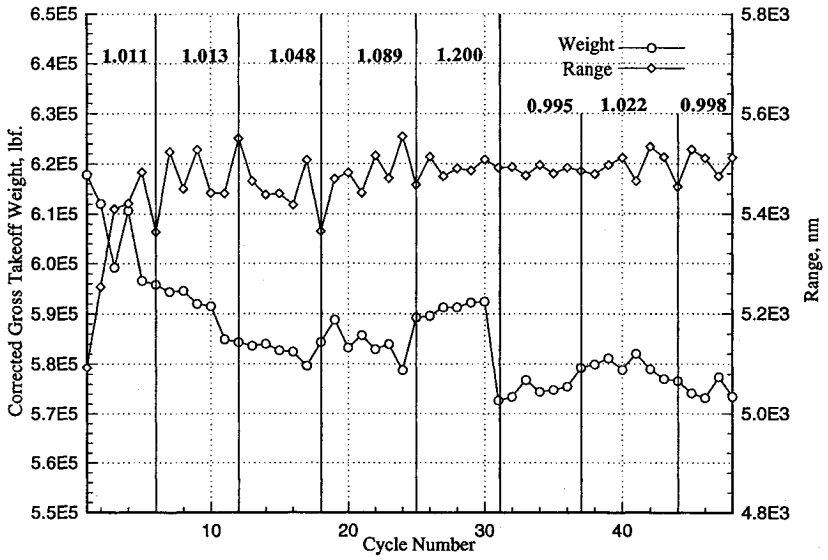


**Fig. 10 Convergence history, case 1.**

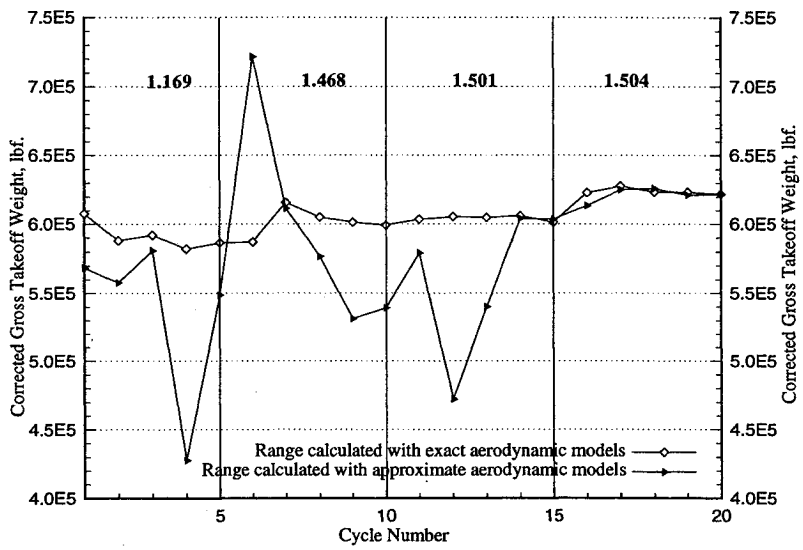


**Fig. 11 Convergence history, case 2.**

This may be seen in the relatively large interlacing factor comparing the FLOPS and the finite element wing weights.

Figures 10 and 11 give the convergence histories of the total takeoff gross weight, the range and the interlacing factors. The interlacing factor in the first case remained close to 1.0, moving only once as far as 1.2. In the second case, the interlacing factor quickly approached 1.5 and remained near there, which mirrors the evolution of the planform. From Fig. 11, it can be seen that the space into which the optimizer moved was one in which the FLOPS weight equation was not particularly good, and as the interlacing factor increased, it became worse. The failure of the optimizer to move out of this region may be because of the local minima created by noisy aerodynamic response and the lack of derivative information for the interlacing factor.

## Conclusions

A finite element model-based structural optimization procedure was successfully implemented to provide accurate estimation of the wing bending-material weight. The results of the structural optimization were compared with estimates from two weight equations. The comparison indicates that the simple weight equations are good at predicting the average structural weight and effects of airfoil thickness on structural weight, but may not model accurately all of the effects of planform changes on the structural weight. The FLOPS weight equation was found to agree with structural optimization much better than the Grumman weight equation. Static aeroelastic effects on wing bending-material weight were found to be small in our HSCT designs.

We have demonstrated a strategy of interlacing aerodynamic and structural optimization efficiently in the design of the HSCT. This strategy used the result of a structural optimization, performed periodically, to scale the statistics-based weight equation in the course of the aerodynamic optimization. Two studies were performed, each with a design that was optimized with and without the interlacing procedure. The results indicate that the interlacing procedure was successful in terms of obtaining designs reflecting a realistic weight estimation. However, the procedure did not protect the design from getting stuck in regions of the design space where the simple weight model was too optimistic. The derivatives of the interlacing scale factors may need to be used to let the aerodynamic optimizer escape domains where the weight equation is inaccurate.

## Acknowledgments

This work was supported by the NASA Langley Research Center under Grant NAG-1-1160 and the National Science Foundation under Grant DDM-9008451. The authors acknowl-

edge the contribution of J. Cruz to the development of the aeroelastic formulation and related computer program.

## References

[1]Unger, E. R., Hutchison, M. G., Rais-Rohani, M., Haftka, R. T., and Grossman, B., "Variable Complexity Interdisciplinary Design of a Transport Wing," *International Journal of Systems Automation Research and Application*, Vol. 2, No. 2, 1992, pp. 87–113.

[2]Hutchison, M. G., Unger, E. R., Mason, W. H., Grossman, B., and Haftka, R. T., "Variable-Complexity Aerodynamic Optimization of an HSCT Wing Using Structural Wing-Weight Equations," *Journal of Aircraft*, Vol. 31, No. 1, 1994, pp. 110–116.

[3]Hutchison, M. G., Huang, X., Mason, W., Haftka, R. T., and Grossman, B., "Variable-Complexity Aerodynamic-Structural Design of a High-Speed Civil Transport Wing," *Proceedings of the AIAA/NASA/USA/ISSMO 4th Symposium on Multidisciplinary Analysis and Optimization*, AIAA, Washington, DC, 1992 (AIAA Paper 92-4695).

[4]Hutchison, M. G., Mason, W., Grossman, B., and Haftka, R. T., "Aerodynamic Optimization of an HSCT Configuration Using Variable-Complexity Modeling," AIAA Paper 93-0101, Jan. 1993.

[5]Torenbeek, E., "Development and Application of a Comprehensive, Design-Sensitive Weight Prediction Method for Wing Structures of Transport Category Aircraft," Delft Univ. of Technology, Rept. LR-693, Delft, The Netherlands, Sept. 1992.

[6]Huang, X., Haftka, R. T., Grossman, B., and Mason, W., "Comparison of Statistical-Based Weight Equations with Structural Optimization for Supersonic Transport Wings," *Proceedings of the AIAA/NASA/USA/ISSMO 5th Symposium on Multidisciplinary Analysis and Optimization*, AIAA, Washington, DC, 1994, pp. 1125–1144 (AIAA Paper 94-4379).

[7]McCullers, L. A., "Aircraft Configuration Optimization Including Optimized Flight Profiles," *Proceedings of a Symposium on Recent Experiences in Multidisciplinary Analysis and Optimization*, compiled by J. Sobieski, 1984, pp. 395–412.

[8]York, P., and Labell, R., "Aircraft Wing Weight Build-Up Methodology with Modification for Materials and Construction Techniques," NASA CR-166173, Sept. 1980.

[9]Craidon, C. B., "Description of a Digital Computer Program for Airplane Configuration Plots," NASA TM X-2074, 1970.

[10]Harris, Roy, V., Jr., "An Analysis and Correlation of Aircraft Wave Drag," NASA TM X-947, 1964.

[11]Carlson, H. W., and Mack, R. J., "Estimation of Leading-Edge Thrust for Supersonic Wings of Arbitrary Planforms," NASA TP 1270, Oct. 1978.

[12]Grandhi, R. V., Thereja, R., and Haftka, R. T., "NEWSUMT-A: A General Purpose Program for Constrained Optimization Using Constraint Approximations," *Journal of Mechanisms, Transmissions and Automation in Design*, Vol. 107, March 1985, pp. 94–99.

[13]Whestone, W. D., "Engineering Analysis Language Reference Manual," Engineering Information System, Inc., July 1983.

[14]Barthelemy, J.-F. M., Wrenn, G. A., Dovi, A. R., Coen, P. G., and Hall, L. E., "Supersonic Transport Wing Minimum Weight Design Integrating Aerodynamics and Structures," *Journal of Aircraft*, Vol. 31, No. 2, 1994, pp. 330–338.

[15]Carlson, H. W., and Mann, M. J., "Survey and Analysis of Research on Supersonic Drag-Due-to Lift Minimization with Recommendations for Wing Design," NASA TP 3202, Sept. 1992.

[16]Giunta, A., Dudley, J., Grossman, B., Haftka, R. T., Mason, W., and Watson, L. T., "Noisy Aerodynamic Response and Smooth Approximations in HSCT Design," *Proceedings of the 5th AIAA/NASA/USA/ISSMO Symposium on Multidisciplinary Analysis and Optimization*, AIAA, Washington, DC, 1994, pp. 1129–1134 (AIAA Paper 94-4377).